JACS
JOURNAL OF THE AMERICAN CHEMICAL SOCIETY

Subscriber access provided by American Chemical Society

Article

MCM-48-like Large Mesoporous Silicas with Tailored Pore Structure: Facile Synthesis Domain in a Ternary Triblock Copolymer–Butanol–Water System

Tae-Wan Kim, Freddy Kleitz, Blain Paul, and Ryong Ryoo

J. Am. Chem. Soc., **2005**, 127 (20), 7601-7610• DOI: 10.1021/ja042601m • Publication Date (Web): 27 April 2005

Downloaded from http://pubs.acs.org on March 25, 2009

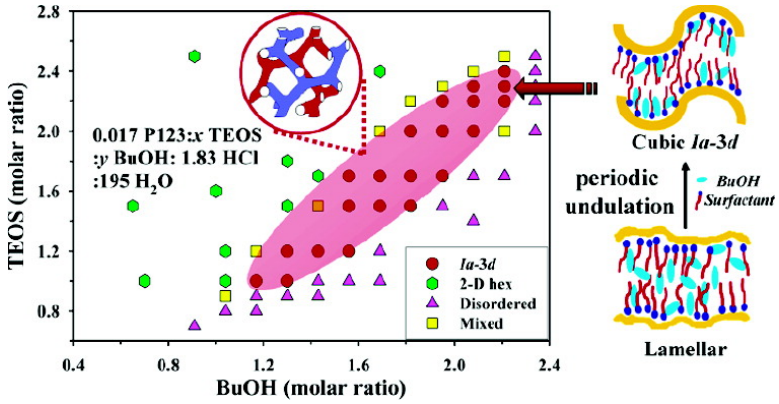

More About This Article

Additional resources and features associated with this article are available within the HTML version:

- Supporting Information
- Links to the 37 articles that cite this article, as of the time of this article download
- Access to high resolution figures
- Links to articles and content related to this article
- Copyright permission to reproduce figures and/or text from this article

View the Full Text HTML

ACS Publications
High quality. High impact.

Journal of the American Chemical Society is published by the American Chemical Society. 1155 Sixteenth Street N.W., Washington, DC 20036

J|A|C|S
ARTICLES
Published on Web 04/27/2005

MCM-48-like Large Mesoporous Silicas with Tailored Pore Structure: Facile Synthesis Domain in a Ternary Triblock Copolymer−Butanol−Water System

Tae-Wan Kim, Freddy Kleitz,‡ Blain Paul, and Ryong Ryoo*

Contribution from the National Creative Research Initiative Center for Functional Nanomaterials, Department of Chemistry (School of Molecular Science-BK21), Korea Advanced Institute of Science and Technology, Daejeon, 305-701 Republic of Korea

Received December 9, 2004; E-mail: rryoo@kaist.ac.kr

Abstract: Assembly of mesostructured silica using Pluronic P123 triblock copolymer ($EO_{20}-PO_{70}-EO_{20}$) and *n*-butanol mixture is a facile synthesis route to the MCM-48-like ordered large mesoporous silicas with the cubic $Ia\bar{3}d$ mesostructure. The cubic phase domain is remarkably extended by controlling the amounts of butanol and silica source correspondingly. The extended phase domain allows synthesis of the mesoporous silicas with various structural characteristics. Characterization by powder X-ray diffraction, nitrogen physisorption, scanning electron microscopy, and transmission electron microscopy reveals that the cubic $Ia\bar{3}d$ materials possess high specific surface areas, high pore volumes, and readily tunable pore diameters in narrow distribution of sizes ranging from 4 to 12 nm. Moreover, generation of complementary pores between the two chiral channels in the gyroid $Ia\bar{3}d$ structure can be controlled systematically depending on synthesis conditions. Carbon replicas, using sucrose as the carbon precursor, are obtained with either the same $Ia\bar{3}d$ structure or $I4_1/a$ (or lower symmetry), depending on the controlled synthesis conditions for silica. Thus, the present discovery of the extended phase domain leads to facile synthesis of the cubic $Ia\bar{3}d$ silica with precise structure control, offering vast prospects for future applications of large-pore silica materials with three-dimensional pore interconnectivity.

Introduction

The advent in the early 1990s of ordered mesoporous materials synthesized with supramolecular aggregates of amphiphiles acting as *structure-directing agents* resulted in an intense scientific research activity and opened up exciting prospects in fields as diverse as catalysis, adsorption, separation, sensing, drug delivery, optoelectronics, and for the manufacture of advanced nanostructured materials.[1] In general, ordered mesoporous materials exhibit significant properties, such as large and uniform pore sizes (typically, in the range of 2−30 nm in diameter), high surface area and pore volume, and well-defined pore topologies. Numerous methods are available for the functionalization of the surface and framework,[2] and shape control of the materials into various morphologies is also possible.[3] In addition, it was shown that ordered mesoporous silicas could serve themselves as *hard templates* for the fabrication of nanostructured materials and nonsiliceous mesoporous materials,[1c,4] including highly ordered mesoporous carbons (OMC).[5]

Particularly interesting materials are mesoporous solids with the three-dimensional (3-D) cubic $Ia\bar{3}d$ mesostructure, which consists of two interpenetrating continuous networks of chiral

‡ Present address: Department of Chemistry, Université Laval, St. Foy, Quebec, G1K 7P4, Canada.

(1) For reviews, see: (a) Ciesla, U.; Schüth, F. *Microporous Mesoporous Mater.* **1999**, *27*, 131. (b) Ying, J. Y.; Mehnert, C. P.; Wong, M. S. *Angew. Chem., Int. Ed.* **1999**, *38*, 56. (c) Schüth, F. *Chem. Mater.* **2001**, *13*, 3184. (d) Scott, B. J.; Wirnsberger, G.; Stucky, G. D. *Chem. Mater.* **2001**, *13*, 3140. (e) Schmidt, W.; Schüth, F. *Adv. Mater.* **2002**, *14*, 629. (f) Stein, A. *Adv. Mater.* **2003**, *15*, 763. (g) Taguchi, A.; Schüth, F. *Microporous Mesoporous Mater.* **2004**, *77*, 1.

(2) (a) Wight, A. P.; Davis, M. E. *Chem. Rev.* **2002**, *102*, 3589. (b) Stein, A.; Melde, B. J.; Schroden, R. C. *Adv. Mater.* **2000**, *12*, 1403. (c) Inagaki, S.; Guan, S.; Fukushima, Y.; Ohsuna, T.; Terasaki, O. *Nature* **2002**, *416*, 304.

(3) (a) Lu, Y.; Ganguli, R.; Drewien, C. A.; Anderson, M. T.; Brinker, C. J.; Gong, W.; Guo, Y.; Soyez, H.; Dunn, B.; Huang, M. H.; Zink, J. I. *Nature* **1997**, *389*, 364. (b) Grün, M.; Lauer, I.; Unger, K. K. *Adv. Mater.* **1997**, *9*, 254. (c) Zhao, D.; Yang, P.; Melosh, N.; Feng, J.; Chmelka, B. F.; Stucky, G. D. *Adv. Mater.* **1998**, *10*, 1380. (d) Yang, P.; Zhao, D.; Chmelka, B. F.; Stucky, G. D. *Chem. Mater.* **1998**, *10*, 2033. (e) Miyata, H.; Kuroda, K. *Chem. Mater.* **1999**, *11*, 1609. (f) Boissière, C.; Larbot, A.; Prouzet, E. *Chem. Mater.* **2000**, *12*, 1937. (g) Kleitz, F.; Marlow, F.; Stucky, G. D.; Schüth, F. *Chem. Mater.* **2001**, *13*, 3587. (h) Melosh, N. A.; Davidson, P.; Chmelka, B. F. *J. Am. Chem. Soc.* **2000**, *122*, 823. (i) Grosso, D.; Soler-Illia, G. J. A. A.; Babonneau, F.; Sanchez, C. *Adv. Mater.* **2001**, *13*, 1085.

(4) (a) Ko, C. H.; Ryoo, R. *Chem. Commun.* **1996**, 2467. (b) Shin, H. J.; Ryoo, R.; Liu, Z.; Terasaki, O. *J. Am. Chem. Soc.* **2001**, *123*, 1246. (c) Shin, H. J.; Ko, C. H.; Ryoo, R. *J. Mater. Chem.* **2001**, *11*, 260. (d) Yang, H.; Shi, Q.; Tian, B.; Lu, Q.; Gao, F.; Xie, S.; Fan, J.; Yu, C.; Tu, B.; Zhao, D. *J. Am. Chem. Soc.* **2003**, *125*, 4724. (e) Tian, B. Z.; Liu, X. Y.; Yang, H. F.; Xie, S. H.; Yu, C. Z.; Tu, B.; Zhao, D. Y. *Adv. Mater.* **2003**, *15*, 1370. (f) Laha, S.; Ryoo, R. *Chem. Commun.* **2003**, *17*, 2138−2139. (g) Schüth, F. *Angew. Chem., Int. Ed.* **2003**, *42*, 3604.

(5) (a) Ryoo, R.; Joo, S. H.; Jun, S. *J. Phys. Chem. B* **1999**, *103*, 7743. (b) Lee, J.; Yoon, S.; Hyeon, T.; Oh, S. M.; Kim, K. B. *Chem. Commun.* **1999**, 2177. (c) Jun, S.; Joo, S. H.; Ryoo, R.; Kruk, M.; Jaroniec, M.; Liu, Z.; Ohsuna, T.; Terasaki, O. *J. Am. Chem. Soc.* **2000**, *122*, 10712. (d) Ryoo, R.; Joo, S. H.; Kruk, M.; Jaroniec, M. *Adv. Mater.* **2001**, *13*, 677. (e) Lee, J.; Han, S.; Hyeon, T. *J. Mater. Chem.* **2004**, *14*, 478. (f) Joo, S. H.; Choi, S. J.; Oh, I.; Kwak, J.; Liu, Z.; Terasaki, O.; Ryoo, R. *Nature* **2001**, *412*, 169. (g) Zhang, W.-H.; Liang, C.; Sun, H.; Shen, Z.; Guan, Y.; Ying, P.; Li, C. *Adv. Mater.* **2002**, *14*, 1776. (h) Vix-Guterl, C.; Boulard, S.; Parmentier, J.; Patarin, J.; Werckmann, J. *Chem. Lett.* **2002**, *10*, 1062. (i) Kim, T.-W.; Park, I.-S.; Ryoo, R. *Angew. Chem., Int. Ed.* **2003**, *42*, 4375. (j) Solovyov, L.; Kim, T.-W.; Kleitz, F.; Terasaki, O.; Ryoo, R. *Chem. Mater.* **2004**, *16*, 2274. (k) Lu, A. H.; Kiefer, A.; Schmidt, W.; Schüth, F. *Chem. Mater.* **2004**, *16*, 100.

channels.[6] These enantiomeric pairs of porous channels are known to be separated by an inorganic wall that follows exactly the gyroid (*G*-surface)[7] infinite periodic minimal surface (IPMS).[8,9] This unique 3-D channel network is thought to provide a highly opened porous host with easy and direct access for guest species, thus facilitating inclusion or diffusion throughout the pore channels without pore blockage. While their properties attract increasing attention for potential use as catalyst, adsorbent, host for nanostructures, and *hard templates* for the fabrication of nano-objects, facile synthesis of such mesoporous solids with the cubic $Ia\bar{3}d$ phase remains challenging. The ionic surfactant-directed cubic $Ia\bar{3}d$ siliceous material designated as MCM-48 is obtained under alkaline conditions in a narrow range of compositions and quite high temperatures,[10−13] by the addition of organic additives[14−16] or by employing mixtures of different surfactants as structure-directing agents,[17] for instance. More recently, other mesostructured and mesoporous materials with cubic $Ia\bar{3}d$ mesophase could be obtained under different conditions.[18−21] However, all of these surfactant-directed cubic $Ia\bar{3}d$ MCM-48-type mesoporous materials have relatively small pore sizes (usually below 4 nm in diameter), which could bring limitations for applications dealing with large molecules or the fabrication of nanostructured objects within the pores. Moreover, the small framework wall thickness usually reported for these materials results in poor thermal and hydrothermal stability. Therefore, scientific efforts have been focused on seeking new routes toward more stable and larger pore cubic $Ia\bar{3}d$ mesoporous materials.

Obviously, large-pore materials with the cubic $Ia\bar{3}d$ structure could play a more significant role in material science if their preparation could be more simplified and widely generalized. One possible strategy in that direction is the use of nonionic block copolymers, which have been proven to be very versatile as structure-directing agents for the preparation of various ordered mesoporous materials, such as SBA-15 (2-D hexagonal *p*6*mm* structure) and SBA-16 (cubic $Im\bar{3}m$).[22−30] The mesoporous silicas obtained from block copolymers possess uniform pores above 5 nm in diameter and thick walls, exhibiting high thermal stability and improved hydrothermal stability compared with that of MCM-41.[6] Very recently, new synthesis pathways utilizing block copolymers as structure-directing agents have been proposed for the generation of cubic $Ia\bar{3}d$ materials. Liu et al.[31] reported the preparation of mesoporous silica membranes displaying cubic $Ia\bar{3}d$ structure using the evaporation-induced self-assembly method,[3a,i] with a mixture of tetraethoxysilane (TEOS) and sulfur-containing silane derivatives in ethanol. Subsequently, other methods were disclosed, using addition of NaI salt,[32] co-condensation reaction of TEOS with vinyl-containing silane,[33] or by using a laboratory-designed block copolymer.[34]

Recently, we emphasized the crucial role of low acid concentrations (between 0.1 and 0.5 M) for the facile preparation of high-quality mesoporous silicas using block copolymers.[27,28] We showed that high-quality 2-D hexagonal SBA-15 and phase-pure large cage face-centered cubic mesoporous silica, both with tailored textural properties, are easily synthesized with the Pluronic-type triblock copolymers by adjusting the kinetics of the inorganic−organic mesophase assembly. Shortly after, the utilization of such low acid catalyst concentration conditions, closer to a thermodynamically favored mesophase formation, suggested the use of *cosolute* molecules (*hydrotropic molecule*s) added to the block copolymer−water system in order to enrich the mesophase behavior.[35,36] Using *n*-butanol (BuOH) as a cosolute, we were able to synthesize a high-quality mesoporous silica, designated as KIT-6, with the cubic $Ia\bar{3}d$ structure in high phase purity. However, certain fundamental aspects of the synthesis conditions, compositional ranges, and physicochemical properties still remained to be substantiated. In particular, the successful synthesis conditions were limited to an extremely narrow range of phase domain around TEOS/P123/HCl/H_2O/BuOH = 1/0.017/1.83/195/1.31 in mole ratio. The products exhibited loss of the $Ia\bar{3}d$ structural order even with a slight variation of the amount of butanol or silica source.

In the present work, we discovered that the phase domain for the cubic $Ia\bar{3}d$ mesoporous silica could be greatly extended, whereas the amounts of BuOH and silica source were changed correspondingly. The extended phase domain covering a wide range of TEOS/P123 allowed facile synthesis of the large-pore cubic $Ia\bar{3}d$ silica materials with various structural characteristics. The porous materials were characterized by X-ray diffraction (XRD), N_2 physisorption analysis, scanning electron microscopy (SEM), transmission electron microscopy (TEM), and by using

(6) Beck, J. S.; Vartuli, J. C.; Roth, W. J.; Leonowicz, M. E.; Kresge, C. T.; Schmitt, K. D.; Chu, C. T.-W.; Olson, D. H.; Sheppard, E. W.; McCullen, S. B.; Higgins, J. B.; Schenkler, J. L. *J. Am. Chem. Soc.* **1992**, *114*, 10834.
(7) Schoen, A. H. NASA Technical Note D-5541; NASA: Washington, D.C., 1970.
(8) Alfredsson, V.; Andersson, M. W. *Chem. Mater.* **1996**, *8*, 1141.
(9) Carlsson, A.; Kaneda, M.; Sakamoto, Y.; Terasaki, O.; Ryoo, R.; Joo, S. H. *J. Electron Microsc.* **1999**, *48*, 795.
(10) Monnier, A.; Schüth, F.; Huo, Q. S.; Kumar, D.; Margolese, D. I.; Maxwell, R. S.; Stucky, G. D.; Krishnamurty, M.; Petroff, P.; Firouzi, A.; Janicke, M.; Chmelka, B. F. *Science* **1993**, *261*, 1299.
(11) Vartuli, J. C.; Schmitt, K. D.; Kresge, C. T.; Roth, W. J.; Leonowicz, M. E.; Sheppardt, B.; McCullen, S. B.; Hellring, S. D.; Beck, J. S.; Schenkler, J. L.; Olson, D. H.; Sheppard, E. W. *Chem. Mater.* **1994**, *6*, 2317.
(12) Morey, M. S.; Davidson, A.; Stucky, G. D. *J. Porous Mater.* **1998**, *5*, 195.
(13) Sayari, A. *J. Am. Chem. Soc.* **2000**, *122*, 6504.
(14) Huo, Q.; Margolese, D. I.; Stucky, G. D. *Chem. Mater.* **1996**, *8*, 1147.
(15) Gallis, K. W.; Landry, C. C. *Chem. Mater.* **1997**, *9*, 2035.
(16) Kim, J. M.; Kim, S. K.; Ryoo, R. *Chem. Commun.* **1998**, 259.
(17) (a) Chen, F. X.; Huang, L. M.; Li, Q. Z. *Chem. Mater.* **1997**, *9*, 2685. (b) Ryoo, R.; Joo, S. H.; Kim, J. M. *J. Phys. Chem. B* **1999**, *103*, 7435. (c) Zhao, W.; Li, Q. Z. *Chem. Mater.* **2003**, *15*, 4160.
(18) Che, S.; Kamiya, S.; Terasaki, O.; Tatsumi, T. *J. Am. Chem. Soc.* **2001**, *123*, 12089.
(19) Kleitz, F.; Thomson, S. J.; Liu, Z.; Terasaki, O.; Schüth, F. *Chem. Mater.* **2002**, *14*, 4134.
(20) Trikalitis, P. N.; Rangan, K. K.; Bakas, T.; Kanatzidis, M. G. *J. Am. Chem. Soc.* **2002**, *124*, 12255.
(21) Ogura, M.; Miyoshi, H.; Naik, S. P.; Okubo, T. *J. Am. Chem. Soc.* **2004**, *126*, 10937.
(22) Zhao, D.; Huo, Q.; Feng, J.; Chmelka, B. F.; Stucky, G. D. *J. Am. Chem. Soc.* **1998**, *120*, 6024.
(23) Sakamoto, Y.; Kaneda, M.; Terasaki, O.; Zhao, D.; Kim, J. M.; Stucky, G. D.; Shin, H. J.; Ryoo, R. *Nature* **2000**, *408*, 449.
(24) Yu, C.; Yu, Y.; Zhao, D. *Chem. Commun.* **2000**, 575.
(25) Kipkemboi, P.; Fogden, A.; Alfredsson, V.; Flodström, K. *Langmuir* **2001**, *17*, 5398.
(26) Matos, J. R.; Kruk, M.; Mercuri, L. P.; Jaroniec, M.; Zhao, L.; Kamiyama, T.; Terasaki, O.; Pinnavaia, T. J.; Liu, Y. *J. Am. Chem. Soc.* **2003**, *125*, 821.
(27) Choi, M.; Heo, W.; Kleitz, F.; Ryoo, R. *Chem. Commun.* **2003**, 1340.
(28) Kleitz, F.; Liu, D.; Anilkumar, G. M.; Park, I. S.; Solovyov, L. A.; Shmakov, A. N.; Ryoo, R. *J. Phys. Chem. B* **2003**, *107*, 14296.
(29) Soler-Illia, G. J. A. A.; Crepaldi, E. L.; Grosso, D.; Sanchez, C. *Curr. Opin. Colloid Interface Sci.* **2003**, *8*, 109 and references therein.
(30) Kim, T.-W.; Ryoo, R.; Kruk, M.; Gierszal, K. P.; Jaroniec, M.; Kamiya, S.; Terasaki, O. *J. Phys. Chem. B* **2004**, *108*, 11480.
(31) Liu, X.; Tian, B.; Yu, C.; Gao, F.; Xie, S.; Tu, B.; Che, R.; Peng, L.-M.; Zhao, D. Y. *Angew. Chem., Int. Ed.* **2002**, *41*, 3876.
(32) Flodström, K.; Alfredsson, V.; Källrot, N. *J. Am. Chem. Soc.* **2003**, *125*, 4402.
(33) Wang, Y. Q.; Yang, C. M.; Zibrowius, B.; Spliethoff, B.; Lindén, M.; Schüth, F. *Chem. Mater.* **2003**, *15*, 5029.
(34) Chan, Y. T.; Lin, H.-P.; Mou, C. Y.; Liu, S. T. *Chem. Commun.* **2002**, 2878.
(35) Kleitz, F.; Choi, S. H.; Ryoo, R. *Chem. Commun.* **2003**, 2136.
(36) Kleitz, F.; Solovyov, L. A.; Anilkumar, G. M.; Choi, S. H.; Ryoo, R. *Chem. Commun.* **2004**, 1536.

a carbon replication technique.[27] On the basis of this result, we introduce a synthetic phase diagram as a function of the silica content and BuOH amount. We analyze the effects of the varying compositions of the initial synthesis mixture on physical properties of the materials. Among these results, particularly interesting is that porous bridges connecting the two interpenetrating channel systems in the cubic $Ia\bar{3}d$ structure can be controlled, that is, open or closed, by simple variation of the synthesis conditions. The presence of the porous bridges connecting the two channels, contrary to the separated channels of MCM-48,[5a,37,38] was pointed out in previous works using carbon replication technique.[35,39] The porous bridges occurring with regularity were confirmed through the structure determination by electron crystallography. However, the control of such interconnecting pore system during synthesis remained, so far, challenging.

Experimental Section

Materials. The mesostructured silica materials were prepared under various synthetic conditions using a mixture of poly(alkylene oxide)-based triblock copolymer Pluronic P123 ($EO_{20}PO_{70}EO_{20}$, MW = 5800, Aldrich) and *n*-butanol (Aldrich, 99.4%) as a structure-directing mixture. The silica source was TEOS (ACROS, 98%) or sodium silicate (DC Chemical, Korea, 25 wt % aqueous solution, Si/Na = 1.5). The molar composition of the starting reaction mixture was varied in the range of 0.017 P123/*x* TEOS/*y* BuOH/*z* HCl/195 H_2O, with $x = 1.0-2.4$, $y = 1.31-2.22$, and $z = 1.83-2.75$. The reaction temperature with TEOS was fixed at 308 K, and hydrothermal temperatures were varied from 308 to 403 K. A typical preparation of the large-pore cubic $Ia\bar{3}d$ mesoporous silica, designated as KIT-6, is as follows:[35] 4.0 g of P123 is dissolved in 144 g of distilled water and 7.9 g of 35 wt % HCl solution with stirring at 308 K. After complete dissolution, 4.0 g of BuOH is added at once. After 1 h stirring, 8.6 g of TEOS is added at once to the homogeneous clear solution. This mixture is left under vigorous and constant stirring at 308 K for 24 h. The synthesis is carried out in a closed polypropylene bottle. Subsequently, the mixture is aged at 373 K for 24 h under static conditions (this process is referred to as hydrothermal treatment). The white precipitated product is filtered hot without washing and dried at 373 K for 24 h in air. Surfactant-free mesoporous materials are obtained after a brief ethanol/HCl washing and subsequent calcination at 823 K in air. In another set of experiments, the hydrothermal treatment temperature, under static conditions following the initial reaction at 308 K, was varied from 308 to 403 K.

The synthesis described above may be carried out in a much larger batch, using for instance, 64 g of P123 in 2.3 L of aqueous solution. Alternatively, cubic $Ia\bar{3}d$ materials can identically be synthesized with sodium silicate as the silica precursor. For this synthesis, sodium silicate (25 wt % aqueous solution, Si/Na =1.5) was used with BuOH/P123 = 1.2 in wt ratio, and the initial reaction temperature was set to 298 K before the hydrothermal heating. Typically, 6 g of P123 is dissolved in 144 g of distilled water and 16.1 g of 35 wt % HCl solution with stirring at 298 K. After complete dissolution, 7.2 g of BuOH is added at once. After 1 h stirring, 74.5 g of sodium silicate 5 wt % solution (diluted from 25 wt %) is added at once to the homogeneous solution. This mixture is left under vigorous stirring at 298 K for 24 h. The mixture is then aged at 373 K for 24 h under static conditions. For the sodium silicate-based synthesis, hydrothermal aging can be performed at temperatures as high as 423 K during 24 h.

Carbon replicas were prepared using KIT-6 silicas as the template and sucrose as the carbon precursor. The synthetic details for the carbon materials followed the procedures described elsewhere for carbon syntheses using MCM-48 and SBA-15, but the amount of the carbon source was adjusted in proportion to the total pore volume of the parent silica templates.[5a,c] Typically, calcined KIT-6 silica was impregnated with an aqueous solution of sucrose containing sulfuric acid. The mixture was placed in a drying oven for 6 h at 373 K, and subsequently, the oven temperature was increased to 433 K and maintained there for 6 h. Sucrose was impregnated once again, and the resultant mixture was treated at 373 and 433 K. The carbonization was completed in a designed quartz reactor with a capillary cap by pyrolysis with heating to 1173 K under atmospheric pressure. The resultant carbon/silica composite was washed with HF solution (10% in water/ethanol mixture).

Measurements. XRD patterns were recorded on a Rigaku Multiplex instrument operated at 1.5 kW, using Cu Kα radiation. Synchrotron powder XRD data were collected using BL8C2 at Pohang Light Source in the reflection mode ($\lambda = 0.154250$ nm). The nitrogen adsorption isotherms were measured at liquid nitrogen temperature (77 K) using a Quantachrome Autosorb-1MP volumetric adsorption analyzer. Before the measurements, silica samples were outgassed under vacuum for 12 h at 473 K. The Brunauer−Emmett−Teller (BET) equation was used to calculate the apparent surface area from adsorption data obtained at P/P_0 between 0.05 and 0.2. The total volume of micro- and mesopores was calculated from the amount of nitrogen adsorbed at $P/P_0 = 0.95$, assuming that adsorption on the external surface was negligible compared to adsorption in pores. The pore size distributions (PSD) were calculated by analyzing the adsorption branch of the N_2 sorption isotherm using the Barret−Joyner−Halenda (BJH) method. Nonlocal density functional theory (NLDFT) analyses were performed to evaluate surface areas, pore volumes, and pore sizes.[40−42] For the analyses, the kernel of NLDFT equilibrium capillary condensation isotherms of N_2 at 77 K on silica was selected for the model isotherms (using desorption branch, and assuming cylindrical pores). Both the BJH and the DFT models were chosen to obtain values from two independent methods. The absolute accuracy of each model for the pore size distributions remains to be determined for the cubic $Ia\bar{3}d$ materials and requires further comprehensive investigations. However, a relative comparison of the values can be performed for each method considering the error of the models as being systematic. SEM images were obtained with a field emission Philips SEM-535M microscope operating at 20 kV. The silica samples were coated with gold before SEM measurement. TEM images were taken from thin edges of particles supported on a porous carbon grid, using JEOL JEM-3010 equipment operated at 300 kV.

Results

Powder XRD patterns of surfactant-free mesoporous silicas are depicted in Figure 1, demonstrating the crucial role of the HCl concentration on the structure of the mesophase formed. The materials presented are synthesized with the hydrothermal treatment performed at 373 K for 24 h and the molar ratios of P123/TEOS/BuOH = 0.017/1.2/1.31, with varying HCl concentration. From the evolution of the diffraction patterns, it is clearly seen that the cubic $Ia\bar{3}d$ phase is formed in the presence of butanol exclusively if the concentration of the acid catalyst is decreased to as low as 0.75 M, with the other synthetic parameters remaining constant. Higher concentrations afford 2-D hexagonal SBA-15-type mesoporous materials. Synthesis in the range of 0.25−0.75 M HCl gives high yields of highly ordered cubic mesoporous silica, close to 100% on the basis of silica recovery. The preparation method has the advantage of being

(37) Kaneda, M.; Tsubakiyama, T.; Carlsson, A.; Sakamoto, Y.; Ohsuna, T.; Terasaki, O.; Joo, S. H.; Ryoo, R. *J. Phys. Chem. B* **2002**, *106*, 1256.
(38) Solovyov, L. A.; Zaikovskii, V. I.; Shmakov, A. N.; Belousov, O. V.; Ryoo, R. *J. Phys. Chem. B* **2002**, *106*, 12198.
(39) Sakamoto, Y.; Kim, T.-W.; Ryoo, R.; Terasaki, O. *Angew. Chem., Int. Ed.* **2004**, *43*, 5231.
(40) Ravikovitch, P. I.; Neimark, A. V. *J. Phys. Chem. B* **2001**, *105*, 6817.
(41) Ravikovitch, P. I.; Neimark, A. V. *Colloids Surf. A: Phys. Eng. Aspects* **2001**, *187*, 11.
(42) Thommes, M.; Köhn, R.; Fröba, M. *Appl. Surf. Sci.* **2002**, *196*, 239.

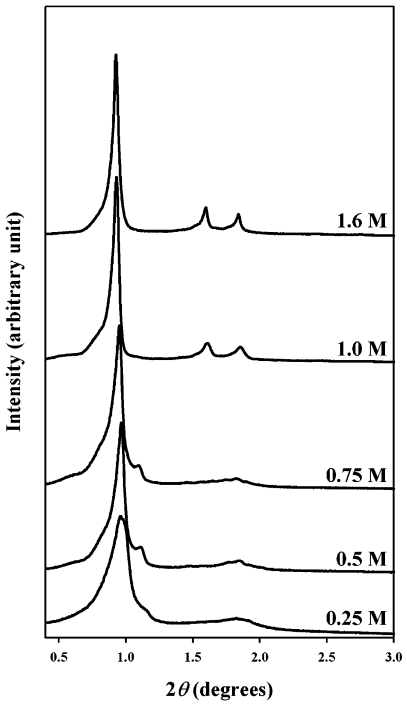

Figure 1. Powder XRD patterns for the mesostructured silica materials obtained using 0.017 P123/1.2 TEOS/1.31 BuOH/*x* HCl/195 H_2O. The molar ratio of HCl (*x*) was varied at $x = 0.915$, 1.83, 2.75, 3.66, and 5.856, giving [HCl] = 0.25, 0.50, 0.75, 1.0, and 1.6, respectively.

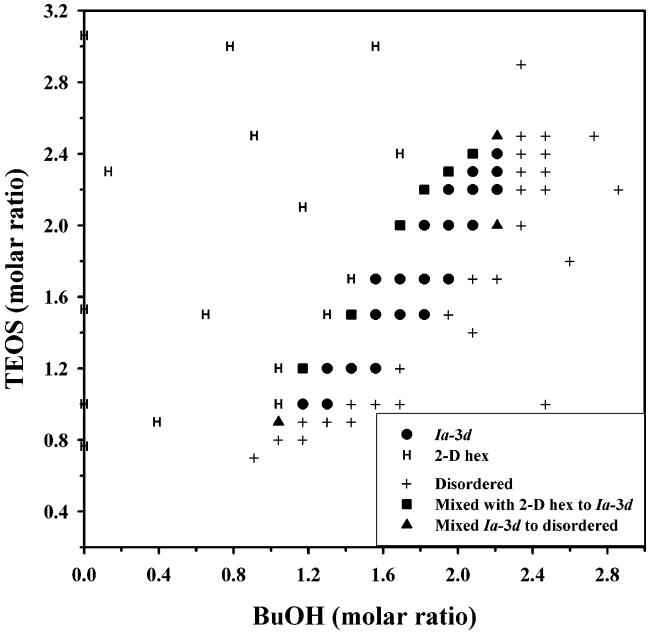

Figure 2. Phase diagram of mesophase structures established according to the XRD measurements. Each sample is prepared with a molar ratio of 0.017 P123/*x* TEOS/*y* BuOH/1.83 HCl/195 H_2O.

simple and highly reproducible in large quantities. The XRD patterns of the cubic mesoporous materials indicate excellent structural order with the symmetry being commensurate with the body-centered cubic $Ia\bar{3}d$ space group. The exact assignment to the $Ia\bar{3}d$ symmetry was confirmed separately by transmission electron microscopy and electron crystallography investigations and reported elsewhere.[35,39] Noteworthy, highly resolved XRD patterns and the electron microscopy studies suggest no structural distortion, different from what was concluded for other related cubic mesophases (designated as FDU-5).[31,46] The unit cell size, calculated from the (211) reflection of the cubic $Ia\bar{3}d$ phase, is measured to be 22.4 nm for the calcined materials obtained at 0.5 M (TEOS/BuOH = 1.2/1.31, at 373 K), a value substantially larger than that of the unit cell parameter of tetraalkylammonium-based cubic analogues (e.g., MCM-48 and related materials).[10−21] One can additionally note a decrease in the *d*-spacing of the main diffraction peaks upon comparing the XRD pattern of the 2-D hexagonal phase obtained at 1.0 M HCl ($d_{100} = 9.5$ nm) and the cubic $Ia\bar{3}d$ one at 0.75 M ($d_{211} =$ 9.3 nm). Such observable changes in position with a small change in HCl concentration are expected when mesophase transition occurs.[43−46] Well-developed cubic $Ia\bar{3}d$ mesophases are obtained when the syntheses are performed at 0.5 M HCl, the latter being the concentration employed to synthesize the materials described in the following text.

The cubic $Ia\bar{3}d$ phase is readily obtainable in a wide range of composition by varying the initial amounts of BuOH and TEOS that are added to the P123−HCl−H_2O system (at 0.5 M HCl). By changing simultaneously these two synthetic variables, we have been able to map the phases that can be generated in the systems, resulting in a detailed synthesis product phase diagram as a function of the amounts of silica source and BuOH (see Figure 2). For this phase diagram, all syntheses were performed at a reaction temperature of 308 K, and the subsequent aging temperature was 373 K. The amount of BuOH added to the synthesis is decisive for the nature of the mesophase. As it can be seen, the region, where a well-developed cubic $Ia\bar{3}d$ phase is obtained, is situated between a large region of 2-D hexagonal mesophase and a region where a less-ordered phase is produced. This poorly ordered phase exhibiting one main broad diffraction peak has not been further characterized. The phase region for the gyroid $Ia\bar{3}d$ structure is highly reproducible and thus well defined, indicating an approximately linear relationship between the amounts of BuOH and TEOS. The interval ratios where the $Ia\bar{3}d$ phase forms are P123/TEOS/BuOH = 0.017/1.0−2.4/1.2−2.2 in molar ratio. At a fixed amount of TEOS, increasing amounts of BuOH added to the synthesis batch lead to transition from 2-D hexagonal to the cubic $Ia\bar{3}d$ mesophase, to, finally, the disordered phase, through smaller domains of intermediate mixed phases. These features are illustrated in Figure 3 for the case of materials synthesized with a fixed ratio of P123/TEOS/BuOH = 0.017/1.5/*y*, where *y* is varied from 1.31 to 1.97 at 0.5 M HCl. The XRD patterns recorded as a function of the BuOH amount show that the structure evolves from a 2-D hexagonal phase analogous to SBA-15[22] to the cubic $Ia\bar{3}d$ phase as the amount of butanol is increased. Conversely, increasing the amount of the silica source in the system while keeping the BuOH amount constant leads to transition from the poorly ordered phase to the well-ordered $Ia\bar{3}d$ phase to, finally, the 2-D hexagonal phase (see Figure S1 of the Supporting Information for the XRD patterns).

(43) Ågren, P.; Lindén, M.; Rosenholm, J. B.; Schwarzenbacher, R.; Kriechbaum, M.; Amenitsch, H.; Laggner, P.; Blanchard, J.; Schüth, F. *J. Phys. Chem. B* **1999**, *103*, 5943.
(44) Tolbert, S. H.; Landry, C. C.; Stucky, G. D.; Chmelka, B. F.; Norby, P.; Hanson, J. C.; Monnier, A. *Chem. Mater.* **2001**, *13*, 2247.
(45) Kleitz, F.; Blanchard, J.; Ågren, P.; Zibrowius, B.; Schüth, F.; Lindén, M. *Langmuir* **2002**, *18*, 4963.
(46) Tian, B. Z.; Liu, X.; Solovyov, L.; Liu, Z.; Yang, H.; Zhang, Z.; Xie, S.; Zhang, F.; Tu, B.; Yu, C.; Terasaki, O.; Zhao, D. *J. Am. Chem. Soc.* **2004**, *126*, 865.

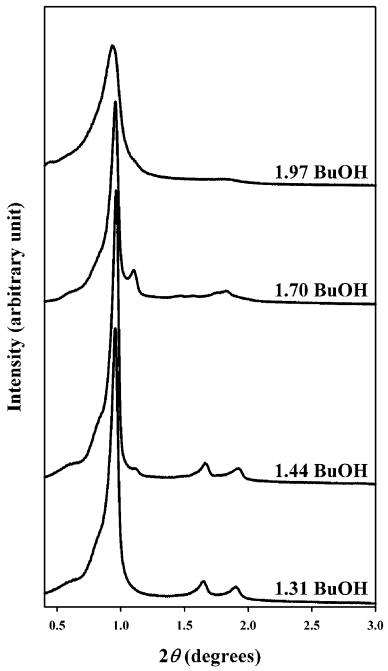

Figure 3. Powder XRD patterns for the mesostructured silica materials obtained using 0.017 P123/1.5 TEOS/*y* BuOH/1.83 HCl/195 H_2O, with various molar ratios of BuOH (*y*).

At high BuOH ($y > 2.2$ in mole ratio), only poorly ordered materials are formed, irrespective of the amount of TEOS employed for the syntheses. Low BuOH ($y < 1$ in mole ratio) yields materials with the 2-D hexagonal phase. Noteworthy, the range, where the cubic $Ia\bar{3}d$ phase is generated, could widely be enlarged compared to our initial communication on the synthesis,[35] in which the cubic phase was described for a fixed molar ratio of P123/TEOS/BuOH = 0.017/1/1.31.

Nitrogen adsorption−desorption isotherms were measured at liquid nitrogen temperature on cubic $Ia\bar{3}d$ samples synthesized according to the gel compositions taken in the cubic phase domain, with concurrent increase of the BuOH and TEOS contents (XRD patterns of the selected silicas are collected in Figure S2, Supporting Information). The resulting sorption isotherms, depicted in Figures S3, obtained for the different calcined samples are all type IV isotherms with a pronounced capillary condensation step, characteristic of high-quality large-pore mesoporous materials. The presence of an H1 hysteresis loop indicates channel-like pores, and the pore size distribution is narrow (Figure S4). In Table 1, the lattice and textural parameters of these representative cubic $Ia\bar{3}d$ porous mesostructured materials synthesized with the addition of BuOH as a co-structure directing agent are summarized. The materials typically synthesized at 373 K have high BET area in the range of 700−800 $m^2\ g^{-1}$ and large pore volume (up to 1 $cm^3\ g^{-1}$). The median pore diameter, as evaluated from the BJH model and DFT calculations, varies between 6.8 and 8.2 nm, strongly depending on the gel composition. As shown in Table 1, an observed trend is the decrease of the mesopore size as the quantities of TEOS and BuOH are increased. This tendency is confirmed by direct observation of the isotherms, where a shift of the position of the capillary condensation toward lower relative pressures occurs (Figure S3).

The hydrothermal treatment was varied between 308 and 403 K for a selected gel composition (0.017 P123/1.2 TEOS/1.31 BuOH/1.83 HCl/195 H_2O) to allow the effective tailoring of the textural parameters of the cubic $Ia\bar{3}d$ KIT-6 silica. The XRD patterns of the materials after calcination at 823 K are reported in Figure 4. The silica samples synthesized at various temperatures all exhibit diffraction patterns characteristic of the cubic $Ia\bar{3}d$ mesostructure. A noticeable increase in the *d*-spacing, and hence, lattice parameters, occurs upon the increase of the temperature applied for the hydrothermal treatment. In addition, one can clearly point to some pronounced differences in the relative peak intensities between the first diffraction peaks of the cubic $Ia\bar{3}d$ phase and the diffraction peaks at higher 2θ angles with increasing treatment temperature, while retaining a high degree of mesoscopic ordering. Figures 5 and 6 show the nitrogen sorption isotherms and pore size distributions, respectively, for the same series of samples. The sorption isotherms for the different calcined samples remain type IV isotherms, similar to SBA-15-type materials,[22,25,27,40] with a sharp capillary

Table 1. Structural Parameters of the Cubic $Ia\bar{3}d$ Mesoporous Silicas which were Prepared as the Molar Ratio of 0.017 P123/*x* TEOS/*y* BuOH/1.83 HCl/195 H_2O[a]

[*x*, *y*]	*a* (nm)	S_{BET} ($m^2\ g^{-1}$)	S_{DFT} ($m^2\ g^{-1}$)	V_t ($cm^3\ g^{-1}$)	V_{DFT} ($cm^3\ g^{-1}$)	w_{BJHads} (nm)	w_{DFT} (nm)	d_s[b] (nm)
[1.0, 1.31][c]	22.7	784	724	0.94	0.92	8.2	8.1	3.2
[1.2, 1.44]	22.4	725	683	0.93	0.91	7.6	7.9	3.3
[1.5, 1.70]	22.4	753	704	0.92	0.91	7.3	7.6	3.6
[2.0, 2.03]	22.4	753	699	0.82	0.82	6.4	7.1	4.2
[2.4, 2.22]	21.6	778	704	0.83	0.81	6.1	6.8	4.0

[a] XRD unit cell parameter (*a*) is equal to $6^{1/2}d_{211}$; S_{BET} is the apparent BET specific surface area deduced from the isotherm analysis in the relative pressure range of 0.05−0.20; V_t is the total pore volume at relative pressure 0.95; w_{BJH} is the pore diameter calculated using the BJH method. S_{DFT} is the specific surface area; V_{DFT} is the total pore volume, and w_{DFT} is the mesopore diameter, calculated by DFT method using the kernel of NLDFT equilibrium capillary condensation isotherms of N_2 at 77 K on silica. [b] The wall thickness (d_s) evaluated by geometrical model, $d_s = a/2 - w_{DFT}$ (ref 38). [c] Sample synthesized following the conditions reported initially, with P123/BuOH = 1:1 (wt %) (ref 35).

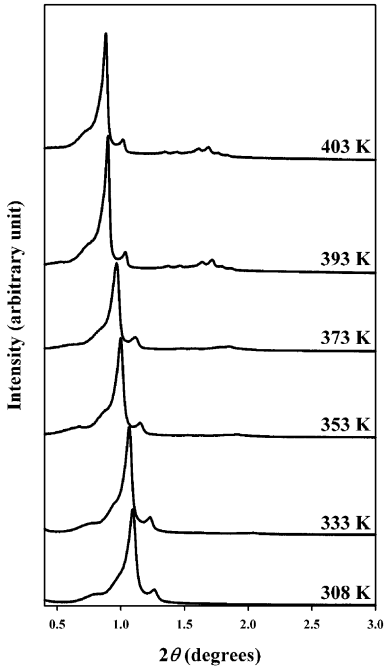

Figure 4. Powder XRD patterns for cubic $Ia\bar{3}d$ KIT-6 silica samples synthesized using 0.017 P123/1.2 TEOS/1.31 BuOH/1.83 HCl/195 H_2O, with various hydrothermal treatment temperatures.

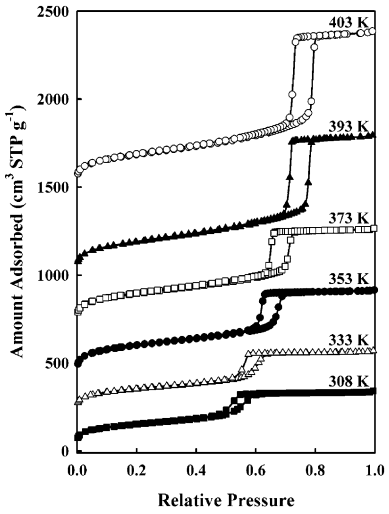

Figure 5. N_2 adsorption−desorption isotherms for cubic $Ia\bar{3}d$ KIT-6 silica samples synthesized at different hydrothermal treatment temperatures, with the composition of 0.017 P123/1.2 TEOS/1.31 BuOH/1.83 HCl/195 H_2O. The isotherms for 333, 353, 373, 393, and 403 K are offset vertically by 200, 400, 700, 1000, and 1500 cm^3 STP g^{-1}, respectively.

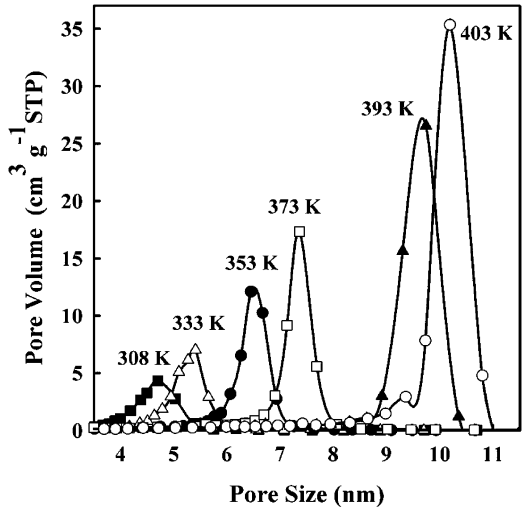

Figure 6. Pore size distributions of mesoporous KIT-6 silicas synthesized at different hydrothermal treatment temperatures. The pore size was analyzed with the adsorption branch using the BJH algorithm (see Figure 5 for sample composition).

condensation step indicative of mesopores narrowly distributed in size, irrespective of the temperature. The shift of the capillary condensation step to higher relative pressure with increasing temperature evidences an increase in the mesopore size, also indicated by the evolving pore size distribution curves. Structural and textural properties are summarized in Table 2 for the samples prepared at various temperatures. The pore volumes are shown to increase significantly, and the pore sizes range from 4.5 to 10 nm for this series of samples. The lattice parameter of the cubic mesophase increases from 19.8 nm at 308 K up to 24.6 nm for the mesoporous materials prepared at 403 K. Moreover, the wall thickness evaluated using a geometrical model[38] is shown to decrease markedly with increasing aging temperature. It has to be noted that the lattice and textural parameters may vary substantially depending on the starting mixture composition, but the same trends of pore size and volume expansion are observed. For instance, pore size up to 12 nm and pore volume reaching 1.1 cm^3 g^{-1} could be obtained

Table 2. Effects of Hydrothermal Treatment on the Structure of Cubic $Ia\bar{3}d$ Mesoporous Silicas

T^a (K)	a (nm)	S_{BET} (m^2 g^{-1})	S_{DFT} (m^2 g^{-1})	V_t (cm^3 g^{-1})	V_{DFT} (cm^3 g^{-1})	w_{BJHads} (nm)	w_{DFT} (nm)	d_s (nm)
308	19.8	536	557	0.51	0.50	4.7	5.7	4.2
333	20.3	537	552	0.56	0.55	5.4	6.1	4.1
353	21.7	713	707	0.79	0.76	6.4	7.0	3.8
373	22.4	702	670	0.86	0.84	7.3	7.6	3.6
393	24.1	680	585	1.21	1.18	9.7	9.4	2.6
403	24.6	671	583	1.34	1.32	10.1	9.8	2.5

[a] T is temperature, at which the reaction mixture was aged for 24 h after synthesis at 308 K, with the molar ratios of 0.017 P123/1.2 TEOS/1.31 BuOH/1.83 HCl/195 H_2O; see Table 1 for other notations.

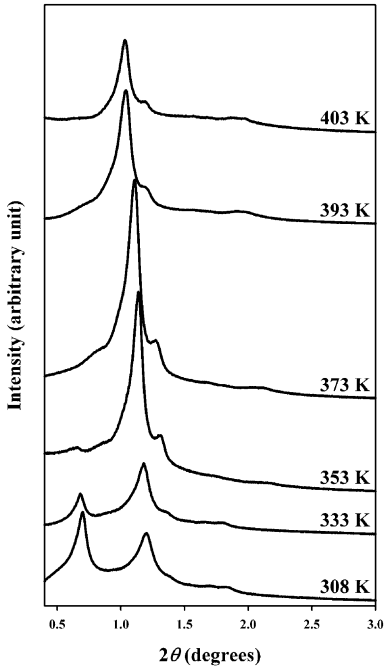

Figure 7. Powder XRD patterns for cubic mesoporous carbon replicas with rod-type nanostructures prepared from cubic $Ia\bar{3}d$ KIT-6 mesoporous silicas synthesized at different temperatures.

for materials with the following gel composition (0.017 P123/1.0 TEOS/1.31 BuOH/1.83 HCl/195 H_2O), when subjected to a hydrothermal treatment at 403 K.[35] Evidently, our synthesis method is unique to permit such a systematic and simple control of the pore dimensions of the large-pore cubic $Ia\bar{3}d$ silica, by simply increasing the aging temperature, among known synthesis recipes for the cubic $Ia\bar{3}d$ large-pore silica.[31−34]

The nature of the pore interconnectivity of the large-pore cubic $Ia\bar{3}d$ silica materials can be ascertained by using inverse carbon replication as a characterization method. Mesoporous silicas synthesized in the presence of the Pluronic-type block copolymers are suitable as hard templates for the synthesis of ordered mesoporous carbons.[5] The CMK-type carbon replicas were thus synthesized using the series of cubic mesoporous silicas prepared at temperatures ranging from 308 to 403 K, with sucrose as the carbon precursor, and characterized by powder XRD. As illustrated in Figure 7, the structural symmetry of the cubic $Ia\bar{3}d$ KIT-6 template was preserved after carbon replication when KIT-6 templates prepared with aging temperatures above 343 K are employed, whereas structurally transformed mesoporous carbon structures, similar to CMK-1, could be produced using KIT-6 templates synthesized at the lower temperatures, ranging from 308 to 333 K. The structure

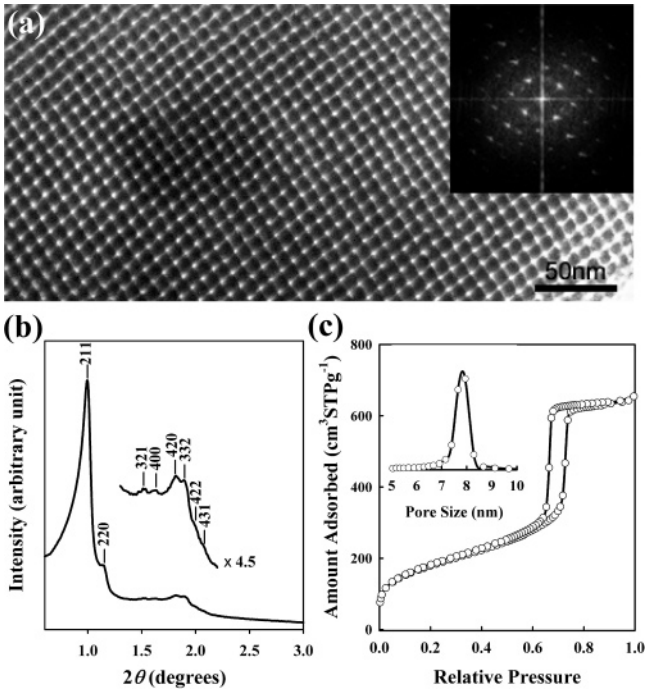

Figure 8. (a) TEM image taken along [531] incidence for a calcined cubic *Ia*$\bar{3}$*d* (KIT-6) silica sample prepared with P123/butanol as the structure-directing mixture and sodium silicate as the silica source, with the hydrothermal treatment performed at 373 K. (b) Powder XRD pattern and (c) N_2 adsorption−desorption isotherm, and respective pore size distribution, for the same cubic KIT-6 sample.

transformation is determined from the presence of the additional reflection below 0.7° 2θ angle.[38] It can be concluded that the two enantiomeric interpenetrating channel networks forming the gyroid structure are independent from each other in the case of KIT-6 materials synthesized at temperatures ranging between 308 and 333 K. At higher treatment temperatures, faithful inverse carbon replicas are produced. This feature could be attributed to the presence of porous bridges or connectivities between the two subsystems of mesoporous channels. Similar effects of temperature are occurring for different starting mixture compositions along the phase diagram, pore size expansion and change in connectivity being general features observed with increasing the aging temperature. However, it is likely that major differences in pore sizes, pore wall thickness, and degree of pore connectivity should be occurring.

Another unique feature of the present synthesis method is that cubic *Ia*$\bar{3}$*d* KIT-6 silica can be synthesized even when sodium silicate is used instead of TEOS. The use of sodium silicate as a cheap silica source is exemplified in Figure 8, and Table 3 lists physicochemical parameters of the cubic *Ia*$\bar{3}$*d* mesoporous silica samples synthesized with sodium silicate as the silica precursor. It is quite remarkable that the synthesis can be performed at a hydrothermal treatment temperature as high as 423 K for 24 h, resulting in materials exhibiting very large pore dimensions and high pore volumes.

Discussion

The synthesis of cubic *Ia*$\bar{3}$*d* large mesoporous silica is based on the use of *n*-butanol in combination with Pluronic P123 ($EO_{20}PO_{70}EO_{20}$) for the structure direction in aqueous solution, at low HCl concentrations. Compared to procedures reported by others,[31−34] the present synthesis approach is very convenient since it can employ cheap reagents, does not depend on batch sizes, and 3-D cubic materials with excellent degree of mesophase ordering are obtained under highly reproducible conditions. Furthermore, we are able to easily tailor the pore dimensions in a wide range, as well as pore connectivity, features that have not been achieved in such a way previously. Large-pore cubic *Ia*$\bar{3}$*d* mesoporous silica is now readily available, similar to its 2-D hexagonal SBA-15 counterpart. In a recent report, we explained that decreasing the HCl concentration is suitable for the production of high-quality mesoporous silicas in high yields with diverse pore structural arrangements.[27,28,35,36] Earlier kinetically controlled pathways are believed to be responsible for synthesis shortcomings. Higher HCl concentrations led to very rapid precipitation of silica, and the details of the mesophase structure were quite difficult to control due to fast reaction kinetics. Now, it is likely that the lower concentrations of the acid catalyst provide more flexibility and facilitate the synthesis of large-pore mesoporous silica in more designed ways. Under these conditions, the phase behavior of the triblock copolymers in water, in the presence of polymerizing silica species, can be sensibly enriched since slower silica condensation kinetics allow the use of cosurfactants or costructure-directing agents to modify *almost thermodynamically* the mesophase. It turned out that the addition of butanol as a *cosolute* and the low HCl concentrations are the prerequisite to obtain the desired cubic *Ia*$\bar{3}$*d* mesophase. Furthermore, the amount of butanol necessary for the formation of the *Ia*$\bar{3}$*d* phase is highly dependent on the initial reagents ratio. The previously reported condition employed a 1:1 wt ratio between P123 and butanol.[35] However, we have realized that it is possible to widely extend the compositional range in which the *Ia*$\bar{3}$*d* phase is found, by increasing initial ratio of the silica source (TEOS) to block copolymers, correspondingly with the increase in the butanol to block copolymer ratio. Increasing the TEOS/P123 ratio is expected to lead to thicker framework walls, similar to what was observed for SBA-15.[27] However, only slight changes in wall thickness are estimated, most likely as a consequence of the presence of butanol in the micelles.

Pore size expansion upon increasing aging temperature is known for other large-pore mesoporous silicas.[22,28,30,47] Our results demonstrate that the aging temperature also serves to influence greatly the porosity of the block copolymer-directed cubic *Ia*$\bar{3}$*d* silicas. At the low HCl concentration, high-quality cubic *Ia*$\bar{3}$*d* phase can be generated with pore diameters ranging from 4 to 12 nm, accompanied by a diminution of the wall thickness, using temperatures from 303 up to 403 K. At low temperatures, the mesopore dimension is most probably deter-

Table 3. Structural Parameters of Cubic *Ia*$\bar{3}$*d* Mesoporous Silicas, Synthesized using Sodium Silicate as the Silica Source

T^a (K)	a (nm)	S_{BET} ($m^2\ g^{-1}$)	S_{DFT} ($m^2\ g^{-1}$)	V_t ($cm^3\ g^{-1}$)	V_{DFT} ($cm^3\ g^{-1}$)	w_{BJHads} (nm)	w_{DFT} (nm)	d_s (nm)
373	22.4	646	566	0.98	0.96	7.9	8.2	3.1
423	23.5	393	392	1.04	0.95	10.0	9.8	2.0

[a] T is temperature, at which the reaction mixture was aged for 24 h after synthesis at 298 K; the 373 K sample was synthesized with the molar ratios of 0.017 P123/1.0 SiO_2/0.34 Na_2O/1.6 BuOH/2.5 HCl/204 H_2O, the 423 K sample with the molar ratios of 0.017 P123/1.2 SiO_2/0.41 Na_2O/1.6 BuOH/2.7 HCl/199 H_2O; see Table 1 for other notations.

(47) Galarneau, A.; Cambon, H.; DiRenzo, F.; Ryoo, R.; Choi, M.; Fajula, F. *New J. Chem.* **2003**, *27*, 73.

mined by the size (or volume) of the hydrophobic polypropylene oxide (PPO) core, while the poly(ethylene oxide) (PEO) chains are protruding into the silica walls. With increasing temperature, the effective volume fraction of the hydrophobic portion of the copolymers increases largely, with the PEO groups becoming more hydrophobic, resulting in wider pores and greater pore volumes. As a consequence of reduced hydration, a shift of the silica region in the micelles is possible, resulting in reducing the silica wall thickness. The PEO groups are believed to segregate toward the hydrophobic volume of the micelles, separating from densifying silica walls, or toward the PEO fraction of adjacent micelles.[47] Since different starting mixtures can be employed, and aging temperature can be tuned finely, tailoring of pore dimensions can be highly precise. Further control of pore dimension could be envisaged by adapting similar synthetic conditions to smaller chain block copolymers, such as Pluronic P103, which has the same volume fraction of EO groups,[32] Brij-type nonionic oligomeric surfactants, or mixtures of these. The variations in the relative intensity of the diffraction peaks of the cubic $Ia\bar{3}d$ phase, occurring with higher aging temperature (Figure 4), can be rationalized by changes in pore diameter relative to pore wall thickness.[27,48,49] The observed evolution of intensity ratio is consistent with widening of the mesopore channels accompanied by a diminishing wall thickness, being also in agreement with the data obtained from N_2 sorption analyses (Table 2).

The structure of KIT-6 may be described by the gyroid IPMS structure with cubic $Ia\bar{3}d$ symmetry,[7,50,51] structurally being similar to smaller-pore MCM-48 silica. The *G*-surface is considered to divide space into two infinite, unconnected but mutually interwoven periodic channel networks. In the case of KIT-6 silica, however, either the enantiomeric pair of interpenetrating 3-D subframeworks of mesoporous channels is interconnected through smaller complementary pores[39,40,47] or the chiral subframeworks can be isolated from each other, depending on the details of synthesis condition. Previously, we confirmed using TEM imaging of platinum nanostructures that the pore shape and connectivity of the cubic $Ia\bar{3}d$ KIT-6 silica can indeed be represented by a pair of interpenetrating networks of channels. The images of the platinum replicas, taken after dissolution of the silica template, revealed extended domains of 3-D Pt nanowire networks, indicating interconnectivity of the silica template. Similarly, the successful preparation of ordered mesoporous carbons from mesoporous silica templates showed that carbon replication is a very useful method for identifying the porous structure of the parent silicas.[5] Using this method, faithful inverse carbon replication was obtained with KIT-6 prepared at temperatures above 343 K. It is worth mentioning that the ordered mesoporous CMK-8 carbons thus obtained exhibit cubic $Ia\bar{3}d$ symmetry with high structural ordering, owing to parent silica templates having complementary pores in the mesopore walls. Recently, Sakamoto et al.[39] investigated the 3-D structure of cubic $Ia\bar{3}d$ KIT-6 silica and the related carbon materials by electron crystallography. The analyses were performed on a cubic $Ia\bar{3}d$ KIT-6 silica sample synthesized at 393 K and its CMK-8 inverse carbon replica. The authors confirmed the presence of complementary pores in the structure of KIT-6 silica and the exact preservation of the cubic $Ia\bar{3}d$ symmetry for the carbon replica. They also suggested regular occurrence of preferential regions for the interconnectivities where minima of silica density are observed. The occurrence of such bridging porosity above 343−353 K may originate from the strong temperature dependency of the triblock copolymer hydration and the high-temperature segregation behavior of the PEO headgroups, combined with silica wall densification and restructuring.[47] Conversely, silica templates obtained at lower temperatures lead to displacement of the two carbon subframeworks, following a CMK-1-type process, which strongly suggests the absence of interconnecting pores between the two mesoporous channel systems.[5a,d] The material designated as CMK-1 was originally prepared using MCM-48 as the template, the latter consisting of two independent interpenetrating channel networks, without connection. Hence, the carbon networks created in the two isolated mesoporous channel systems were not connected and were displaced with respect to one another when the MCM-48 silica template is removed. Consequently, the structure of the resulting CMK-1 carbon was found to change to lower symmetry.[5,38,39] The same effect is observed when KIT-6 silica templates prepared at low temperatures are employed, as it is clearly confirmed by the appearance of the additional diffraction peak below 0.7° 2θ angle (Figure 7). It is, therefore, likely that the periodic structure of the displaced CMK-8 material is different from that of the parent KIT-6 template, as well. Such large-pore CMK-1-like carbon samples may exhibit significantly different textural properties from those of undisplaced CMK-8 carbons and will be the topic of a forthcoming report.

The approach of the synthesis of high-quality large-pore cubic $Ia\bar{3}d$ mesoporous silicas is based on two fundamental aspects: the phase-controlling effect (*thermodynamic*) of butanol in the $SiO_2-EO_{20}PO_{70}EO_{20}-H_2O-HCl$ system on one hand, and the micelle-folding effect (*kinetic*) during silicate polymerization on the other hand. In our case, the formation of the mesophase can be governed more thermodynamically because the concentration of the acid catalyst is decreased. XRD patterns collected at different stages during the reaction showed that the cubic $Ia\bar{3}d$ phase is formed via a structural evolution mechanism (Figure 9). Accordingly, the mechanism seems to involve a transformation from a lamellar phase (Figure 9a), appearing initially after 4−6 h of reaction, depending on the starting mixture composition, to the desired bicontinuous cubic phase (Figure 9c). The combined roles of butanol and low concentrations of acid are essential for this structural evolution. Butanol is known to act as a *cosolute* in block copolymer−water systems, which co-micellizes with the block copolymer and stabilizes polar−apolar interfaces, determining the micellar interfacial curvature. Since butanol is polar, it can interact with both PEO and PPO blocks, with its polar −OH headgroup assumed to be located mostly at the hydrophilic−hydrophobic interface of the micelles.[52,55] We proposed that the addition of butanol produces a pronounced decrease in the interfacial curvature of the micellar system. This effect could be explained on the account of changes in the hydrophobic to hydrophilic volume ratio of the block copolymer micelles, leading first to formation of a mesophase with decreased curvature (lamellar).[43,45,52−55]

(48) Sauer, J.; Marlow, F.; Schüth, F. *Phys. Chem. Chem. Phys.* **2001**, 3, 5579.
(49) Kleitz, F.; Schmidt, W.; Schüth, F. *Microporous Mesoporous Mater.* **2003**, *1*, 65.
(50) Luzzati, V.; Spegt, P. A. *Nature* **1967**, *215*, 701.
(51) Clerc, M.; Dubois-Violette, E. *J. Phys. France II* **1994**, *4*, 275.
(52) Feng, P.; Bu, X.; Pine, D. J. *Langmuir* **2000**, *16*, 5304.

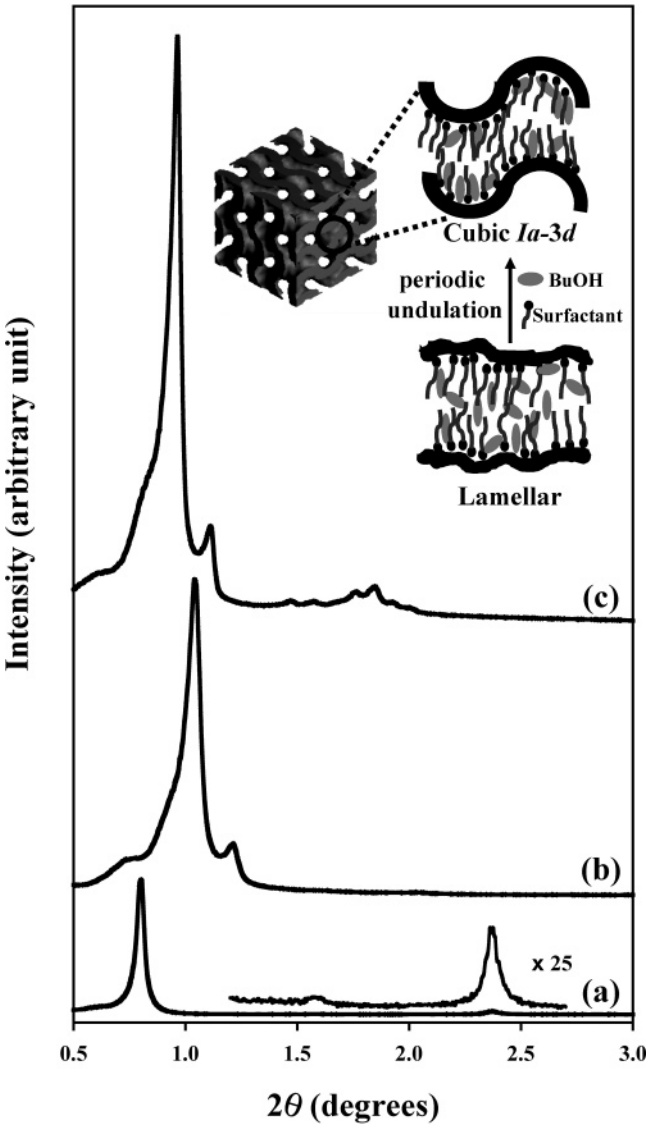

Figure 9. HRXRD patterns for the mesostructure obtained using 0.017 P123/1.2 TEOS/1.31 BuOH/1.83 HCl/195 H_2O during formation of the cubic $Ia\bar{3}d$ phase, as a function of temperature and time: (a) 308 K for 3 h, (b) 308 K for 24 h, and (c) 308 K for 24 h, and subsequently 373 K for 24 h. Inset is a schematic illustration of the lamellar-to-cubic transformation.

Precisely, the addition of TEOS to the BuOH/P123 mixture should result initially in silica−block copolymer micelles with reduced curvature, which eventually aggregate together and coalesce in a lamellar-type silica−block copolymer mesophase. In the absence of BuOH, the higher curvature 2-D hexagonal SBA-15-type mesophase is generally observed. For insights on the mechanism of formation of 2-D hexagonal SBA-15-type mesophases, we refer to the important studies of Lindén and Alfredsson.[56] Moreover, it is possible that the presence of butanol results in reduced hydration of the EO groups, similar to what is observed in ternary triblock copolymer−BuOH−H_2O systems, driving to decreased curvatures.[55b] In other words, the hydrophilic region of the micellar aggregates, which would interact with water and silica species, is most probably smaller than that in the absence of butanol, at least at the early stages of the mesophase formation. Consequently, the interfacial region becomes thinner and more flexible. Possible undulations could be promoted, which may result in deformation of the mesophase ordering during silicate condensation. Here, it is important to keep in mind that in the SiO_2−P123−BuOH−H_2O−HCl system, silica species have a fairly strong hydrogen-bonding capacity with the EO groups, resembling the *hydration* the block copolymer chains. Therefore, time-dependent changes of the thickness of the interfacial region in the presence of silica should be accounted as well. By slowing down the condensation kinetics, it is likely that the silicate species remain quite *soft*, and the less rigid silica oligomers will allow more flexibility for reorganizing the structure and adapting changes in curvature. At early stages, silicate species are loosely condensed with a low degree of cross-linking. Upon further reaction at 308 K, condensation increases progressively in the silicate region, which possibly imposes stress and geometrical frustration, provoking undulations and regular folding of the silica surface. Anisotropic fluctuations in the hybrid mesophase due to silica condensation, facilitated by the flexible interfacial region, induce significant changes in the inorganic−organic interfacial curvature and the subsequent observed change in symmetry leading ultimately to the gyroid IPMS.[51,57] This mechanism can be compared to the mechanism of formation of single crystal-like particles of MCM-48,[16] which occurs more likely by a layer-by-layer crystal growth leading to particles with controlled symmetry and morphology (Figure S5a). Differently, the transformation of a lamellar phase with 1-D ordering into an isotropic cubic phase upon regular fluctuation is not prone to produce crystals with well-defined morphology. Therefore, the morphology of KIT-6 silica particles remains amorphous, as shown in Figure S5b,c. Such a structural transformation via phase transformation was not observed previously for triblock copolymer-based systems. At present, however, additional cosolvent effects caused by minor amounts of butanol solubilized in water[55] cannot be fully excluded. Furthermore, the role of butanol may be time-dependent as ethanol produced by the slow hydrolysis of TEOS is increasingly released into the system, which in turn may induce an increased solubility of butanol. Consequently, a possible change in butanol content could provoke opposite changes in curvature, as well, helping the lamellar-to-cubic $Ia\bar{3}d$ transition. The approach of mixing triblock copolymers and costructure-directing agents has emerged as an elegant alternative strategy for the synthesis of elaborated large-pore mesoporous silicas, compared to the use of salt additions, time-consuming synthesis of new structuring-directing entities, or kinetically dependent co-condensation reactions.

Conclusions

The preparation method for cubic $Ia\bar{3}d$ large mesoporous silicas, which is based on the use of *n*-butanol as a costructure-directing agent with triblock copolymers, is straightforward and highly reproducible, irrespective of the size of the synthesis batch. Furthermore, this method is currently the only available route to cubic $Ia\bar{3}d$ large mesoporous silica allowing the use of

(53) Armstrong, J.; Chowdhry, B.; Mitchell, J.; Beezer, A.; Leharne, S. *J. Phys. Chem.* **1996**, *100*, 1738.
(54) Kwon, K.-W.; Park, M. J.; Hwang, J.; Char, K. *Polym. J.* **2001**, *33*, 404.
(55) (a) Holmqvist, P.; Alexandridis, P.; Lindman, B. *Macromolecules* **1997**, *30*, 6788. (b) Holmqvist, P.; Alexandridis, P.; Lindman, B. *J. Phys. Chem. B* **1998**, *102*, 1149.
(56) (a) Flodström, K.; Teixeira, C. V.; Amenitsch, H.; Alfredsson, V.; Lindén, M. *Langmuir* **2004**, *20*, 4885. (b) Flodström, K.; Wennerström, H.; Alfredsson, V. *Langmuir* **2004**, *20*, 680.
(57) Imai, M.; Kawaguchi, A.; Seaki, A.; Nakaya, K.; Kato, T.; Ito, K.; Ameniya, Y. *Phys. Rev. E* **2000**, *62*, 6865.

a cheap sodium silicate as silica precursor. It has become possible to synthesize the cubic *Ia*$\bar{3}$*d* phase in a wide range of starting mixture compositions, and the first synthetic phase diagram in the $SiO_2-EO_{20}PO_{70}EO_{20}-BuOH-H_2O-HCl$ system is given by the present work. Most importantly, a precise control of the porosity, in particular pore dimensions, was achieved easily by exposing the synthesis mixtures to different aging temperatures. Moreover, the pore network connectivity of the cubic *Ia*$\bar{3}$*d* silica could be tuned, as proven by ordered mesoporous carbon replications. Highly ordered cubic *Ia*$\bar{3}$*d* mesoporous silica with connected pore channels is produced at high hydrothermal treatment temperatures (>343 K), whereas *Ia*$\bar{3}$*d* silicas exhibiting isolated pore systems can be generated at lower temperatures. These silica structures gave two different carbon replicas corresponding to the faithful replication (i.e., cubic *Ia*$\bar{3}$*d*) and the displaced subframeworks ($I4_1/a$ or lower symmetry as in the case of *previous* CMK-1 carbon).

The cubic *Ia*$\bar{3}$*d* silica can be synthesized as easily as the 2-D analogue, SBA-15. Due to the great ease of synthesis, the silica with 3-D channel structure is particularly suitable as reference materials for systematic investigations of adsorption, diffusion, delivery and release, and host−guest interactions. Furthermore, the *Ia*$\bar{3}$*d* silica could be a versatile hard template for the preparation, via *nanocasting*, of new nonsiliceous materials with tailored textural properties with various compositions, such as carbons, metals, metal oxides, and polymers.

The mechanism of the silica formation could be discussed in terms of structural transformation or evolution of the hybrid silica−triblock copolymer mesophase. It is likely that regular undulations could be responsible for the transition from an initially layered mesophase with loosely condensed silicate species to the cubic *Ia*$\bar{3}$*d* phase through ongoing silica polymerization and enhanced cross-linking. Deeper understandings on the mechanism would be useful for the development of synthesis routes to other mesostructured inorganic materials. However, further fundamental investigations and time-resolved studies are still necessary to substantiate the distinct role(s) and location of the organic additive, as well as the nature and resulting effects of the evolving silica species.

Acknowledgment. The work was supported by the Korea Ministry of Science and Technology and the School of Molecular Science through the Brain Korea 21 project. Synchrotron radiation XRD was supported by Pohang Light Source.

Supporting Information Available: HRXRD patterns for the mesostructured silica materials obtained using 0.017 P123/*x* TEOS/1.7 BuOH/1.83 HCl/195 H_2O; HRXRD patterns for the cubic *Ia*$\bar{3}$*d* mesoporous KIT-6 silicas obtained using 0.017 P123/*x* TEOS/*y* BuOH/1.83 HCl/195 H_2O; N_2 adsorption−desorption isotherms for cubic *Ia*$\bar{3}$*d* KIT-6 silica samples; and pore size distributions of mesoporous *Ia*$\bar{3}$*d* KIT-6 silicas. This material is available free of charge via the Internet at http://pubs.acs.org.

JA042601M